Control of Water Distribution Networks with Dynamic DMA Topology Using Strictly Feasible Sequential Convex Programming

Robert Wright[1], Edo Abraham[1], Panos Parpas[2], Ivan Stoianov[1]

Corresponding author: Robert Wright, InfraSense Labs, Dept. of Civil and Environmental Eng., Imperial College London, SW7 2BU, London, UK. (robert.wright07@imperial.ac.uk)

[1]InfraSense Labs, Dept. of Civil and Environmental Eng., Imperial College London SW7 2BU, London, UK.

[2]Dept. of Computing, Imperial College London SW7 2BU, London, UK.

Abstract. The operation of water distribution networks (WDN) with a dynamic topology is a recently pioneered approach for the advanced management of district metered areas (DMA) that integrates novel developments in hydraulic modelling, monitoring, optimization and control. A common practice for leakage management is the sectorization of WDNs into small zones, called DMAs, by permanently closing isolation valves. This facilitates water companies to identify bursts and estimate leakage levels by measuring the inlet flow for each DMA. However, by permanently closing valves, a number of problems have been created including reduced resilience to failure and suboptimal pressure management. By introducing a dynamic topology to these zones, these disadvantages can be eliminated whilst still retaining the DMA structure for leakage monitoring. In this paper, a novel optimization method based on sequential convex programming (SCP) is outlined for the control of a dynamic topology with the objective of reducing average zone pressure (AZP). A key attribute for control optimization is reliable convergence. To achieve this, the SCP method we propose guarantees that each optimization step is strictly feasible, resulting in improved convergence properties. By using a null space algorithm for hydraulic analyses, the computations required are also significantly reduced. The optimized control is actuated on a real WDN operated with a dynamic topology. This unique experimental programme incorporates a number of technologies set up with the objective of investigating pioneering developments in WDN management. Preliminary results

indicate AZP reductions for a dynamic topology of up to 6.5% over optimally controlled fixed topology DMAs.

KeyWords Dynamic Topology, Water Distribution Networks, Optimization, Pressure Management, Flow Modulation

1. Introduction

The installation of District Metered Areas (DMA) is one of the most successful methods that water companies use for identifying and reducing leakage and implementing simplistic pressure management. This involves the segregation of the water distribution network (WDN) into small zones, known as DMAs, by permanently closing isolation valves. Their permanent closure stops flow from breaching the boundary of the DMA and they are therefore commonly referred to as boundary valves (BV). Each DMA typically has a single inlet (feed). The benefits of this approach are as follows:

- During times of low demand (i.e. at night), the flow at the DMA inlet is monitored and leakage estimates are made. This aids in the identification of new bursts as well as prioritization within rehabilitation schemes for DMAs that possess high background leakage.
- Simplistic pressure management can be implemented by installing a pressure reducing valve (PRV) at the DMA inlet. Reducing the average zone pressure (AZP) reduces leakage within the DMA. The pressure reduction must be carried out with a high degree of certainty to ensure customers still receive an adequate level of service i.e. a minimum allowable pressure must be maintained. In order to aid with this, a water company can monitor pressure at the critical point (CP) of the DMA, which is defined as the point of the DMA where pressure is closest to the minimum allowable pressure. Provided that the CP of the DMA does not move, maintaining a minimum allowable pressure at the CP

guarantees that all customers in the DMA have a sufficient level of service. There is also substantial evidence that pressure management reduces future burst frequency (*Lalonde et al.* [2008] and *Fantozzi et al.* [2009] report burst reductions of up to 40% following the implementation of pressure management).

The implementation of DMAs in the UK has successfully facilitated water companies to reduce leakage by 30% over the last 25 years [*Ofwat*, 2007]. Its implementation however has not been without several severe drawbacks due to the permanent closure of the boundary valves, and are summarized as follows:

- Reduced resilience to failure. In this paper, we use redundancy as a measure of resilience to failure [*Yazdani et al.*, 2011]. The permanent closure of boundary valves reduces the network redundancy which results in a reduced number of independent supply routes for consumers. The network is therefore less resilient to failure. For single feed DMAs, more single points of failure exist. In the event of failure, boundary valves are commonly opened manually in order to sustain pressure and keep customers in service [*Drinking Water Inspectorate*, 2009]. The manual opening of boundary valves must be undertaken carefully to avoid the generation of pressure transients that could cause secondary pipe failures. Furthermore, a substantial amount of time is needed to detect the incident, plan a rezone of the DMA, and travel to the affected area in order to open boundary valves, during which time the customer's service is disrupted.
- Suboptimal pressure management due to higher frictional energy losses occurring in single feed DMAs [*Wright et al.*, 2014]. By operating a DMA with multiple sources, new paths exist between demand nodes and source nodes. This increased redundancy generally results in lower frictional energy losses due to the principle of least action [*Piller et al.*,

2003]. Figure 1 demonstrates this process. The total frictional head losses in a WDN model are summed and plotted with the corresponding total instantaneous consumption. Two scenarios are tested, the first has a single source available, and the second has two sources available. All other aspects of the WDN model are identical. The head losses are on average 12.7% lower for the WDN with multiple sources. PRVs can consequently operate with a lower outlet pressure that still maintains pressure at the CP of the network, which is facilitated by the reduction in frictional head losses.

- Water quality incidents due to the build-up of stagnant water at artificially created dead ends [*World Health Organization*, 2004]. This problem is exacerbated when the closed boundary valves need to be opened, such as failure events. This can lead to the customers' water supply becoming discolored and penalties issued by the regulator. The *World Health Organization* [2004] recommends that the artificial implementation of dead ends is limited in the design and operation of WDNs.

The disadvantages of implementing DMAs are now becoming more detrimental as water companies in the UK are facing severe financial penalties for poor customer service from the economic regular, known as Ofwat. These penalties fall under service frameworks such as the Service Incentive Mechanism (SIM, *Ofwat* [2012]) and the Guaranteed Standards Scheme (GSS, *Ofwat* [2008]). The size of the penalties can be as high as 1% of the water company's revenue [*Ofwat*, 2014]. Instances of poor customer service range from low pressures (GSS Regulation 10), stagnant or discoloured water at the customers supply point [*Drinking Water Inspectorate*, 2009], supply failure (GSS Regulation 8 and 9) as well as customers needing to contact their water companies for other reasons related to their service, which they may consider to be unsatisfactory. One example of this is

high variability in diurnal pressure, which affects the perception of a good level of service (personal communications with water companies). Furthermore, water companies are also rewarded up to 0.5% of their revenue for performing well in the SIM framework [*Ofwat*, 2014], adding further incentive to provide a strong level of service. In order to address these new requirements in customer service levels, utilities need to carefully plan mitigations that are also closely linked with addressing the disadvantages of DMAs. Finally, there is still a strong emphasis being placed on further reducing leakage levels.

DMAs with dynamic topology is a novel approach to the operational management of WDNs, where DMAs are dynamically aggregated for improved network resilience, pressure management and water quality, and segregated periodically (e.g. each night, once per week, etc.) for leakage monitoring at night [*Wright et al.*, 2014]. This is facilitated by replacing certain closed boundary valves with self-powered, remote control valves, i.e. dynamic boundary valves (DBV), that incorporate a novel dual bypass pilot system for bidirectional flow and control. The operation of a dynamic DMA topology can therefore successfully eliminates the disadvantages of conventional DMAs, whilst retaining or even improving its success in leakage monitoring, since even smaller DMAs can be set up without introducing the disadvantages associated with permanently closing more boundary valves.

An optimisation method based on sequential convex programming (SCP) was outlined by *Wright et al.* [2014] for the minimisation of network pressure through valve control for both single-feed DMAs and DMAs with a dynamic topology. Although this method showed good convergence properties for both small and large networks, the dynamic aggregation of DMAs can result in the formation of very large and complex networks. Con-

sequently, the SCP method would sometimes have convergence problems. In this paper, it is shown that reliable convergence can always be achieved for the valve control problem by guaranteeing that each iteration of the optimization method is strictly feasible. The resulting optimisation method outlined in this paper is therefore termed Strictly Feasible Sequential Convex Programming (SFSCP). In addition, this paper uses SFSCP for the valve control of a real, operational network for the minimization of AZP. A comparison is then made in this unique experimental investigation between two different types of network configuration, which are each in operation for a 5 day period. The first configuration is a traditional closed, fixed DMA topology, where PRVs are controlled using SFSCP to minimize AZP. The second configuration is a dynamic DMA topology, where the DBVs open during the day for improved pressure management and resilience to failure, and close at night for leakage monitoring activities. The SFSCP algorithm is also used to control the PRVs during the second configuration. Comparisons are then made based on the measured AZP and the total water supplied to the experimental programme network.

The remainder of this paper is structured as follows. In Section 2, the concept of a dynamic DMA topology is detailed, and the experimental programme is described. In Section 3, the development of the proposed SFSCP algorithm is detailed. In Section 4, data demonstrating the actuation of control, AZP, and water use in the experimental programme is presented. Finally, conclusions and future work is detailed in Section 5.

2. DMAs with Dynamic Topology

2.1. Concept

Each DBV incorporates a novel dual bypass pilot system for bidirectional flow and control. This is facilitated by incorporating check valves in each bypass, to ensure only

one bypass is operational at any point in time. The ability to control flow bidirectionally is in contrast to most PRVs, which have a pilot valve on a single bypass, and therefore only facilitate flow and control in a single direction. A PRV will consequently act as a check valve (closed stem position) in the event of a flow reversal. By introducing bidirectional flow and control at the DMA boundary, optimal pressure management and resilience to failure can be achieved. The dynamic DMA topology concept is applicable for the progressive upgrade of networks that already have DMAs installed (for example, the UK where DMAs are ubiquitous), or for networks where DMAs do not exist and require zoning.

The DBVs used in the experimental investigation of this paper also include:

- Advanced pilot controller for open/closed loop control scheduling, stem position control, and flow modulation [*Cla-Val*, 2015a];
- Telecommunications for receiving hydraulic data and updating control settings;
- Insertion flow meter that uses the vortex shedding phenomenon to calculate flow [*Cla-Val*, 2015b], which is beneficial when there are space constraints that restrict the installation of a flow meter at the DBV;
- Micro-turbine for energy harvesting, powered by a valve bypass using the pressure differential of the valve [*Cla-Val*, 2015c], which can be useful when mains power is unavailable;
- High speed (128S/s) pressure measurements at the valve inlet and outlet using the InfraSense TS logger [*Hoskins and Stoianov*, 2014], which is used extensively in the experimental investigation for establishing the AZP performance of the network and guaranteeing that stable (steady-state) control is actuated.

The DBVs add redundancy to the network and reduce the total frictional head losses occurring. By retrofitting PRVs (either existing or newly installed) in the network with the same technology, optimal control can be remotely actuated, and the AZP can be reduced in a way that takes advantage of the reduced head losses that occur, as discussed in Section 1.

Before DMAs are hydraulically connected using the technology outlined above, it is necessary to investigate the potential for negative effects or challenges that might arise as a result of dynamic DMA aggregation. First, the mixing of water from different sources, with a different water quality, can result in consumers receiving water of different qualities at different times. This can cause problems for certain industrial users, where their processes have been calibrated for a certain type of water quality [*World Health Organization*, 2004]. Any industrial users that could be affected by mixing should be consulted before implementing a dynamic DMA topology. In a similar way, residential customers could be affected if they perceive the water to change in quality. Hydraulic modelling and laboratory testing can also be used to ensure customers are not negatively affected by mixing, a process that should be undertaken for any multi-feed WDN [*World Health Organization*, 2004]. Second, contamination can spread further in networks where DMAs do not exist, or where DMAs are hydraulically connected using a dynamic topology. It is important for a water company to carefully balance this risk with the benefits gained from operating a dynamic DMA topology. A valuable step would be collaboration with water companies that do not use DMAs on their network to understand mitigation and incident management related to contamination. Finally, the dynamic aggregation of DMAs complicates the valve control of the network for pressure management compared with single-feed

DMAs. This paper addresses this challenge with the development of the SFSCP algorithm presented in Section 3.

The challenges outlined above should then be compared with the advantages of operating a dynamic DMA topology, which can be summarised as follows:

- Frictional energy losses are reduced due to the increased network redundancy, facilitated by replacing permanently closed boundary valves with DBVs. The reduction in frictional energy losses consequently enables PRVs to operate with lower outlet pressure profiles, which consequently reduces leakage in the network. In order to demonstrate the improvements in pressure management, Section 4 experimentally shows the AZP of dynamically aggregated DMAs and compares this with the same network configured with closed, fixed topology DMAs.
- The resilience to failure of the WDN is substantially improved because multiple supply paths to independent water sources now exist due to the interconnection of DMAs that were previously isolated. In failure situations, these additional supply paths are available immediately and the slow and manual response of opening boundary valves is therefore eliminated. The possibility of knock-on pipe failures due to the potential generation of pressure transients associated with manually opening boundary valves is also eliminated. The resilience to failure of dynamically aggregated DMAs is not discussed further in this paper, but a more in-depth discussion is presented by *Wright et al.* [2014].
- Fewer dead ends at closed boundary valves now exist, therefore there is less stagnant water within the WDN. Opening boundary valves no longer presents a risk of discoloration of the customers' supply. The effects of a dynamic DMA topology on water quality is not

investigated further in this paper, however an extensive investigation into the effects of DMAs on water quality is presented by *Armand et al.* [2015].

By enabling the dynamic reconfiguration of DMAs, WDNs can be operated optimally depending on the hydraulic conditions, and water utilities will be better placed to address the current and future challenges that they face.

2.2. Experimental Programme

In order to investigate the operation of a dynamic DMA topology, an experimental programme is set up on two real, interconnected DMAs. This unique facility combines the installation of the technology discussed in section 2.1 within an operational WDN and facilitates the implementation and investigation of pioneering developments in DMA and WDN management. At present, this WDN is operating with a dynamic topology.

The two DMAs in the experimental programme serve approximately 8,000 properties and are shown in Figure 2 together with an elevation plot. The network graph has 2,374 nodes and 2,434 links. Both DMAs were originally single feed, and separated by multiple closed boundary valves. Each DMA has a separate CP. For most nodes, the minimum allowable pressure set by the water company and regulator is $15mH_2O$, which facilitates aggressive leakage reduction whilst still maintaining minimum service levels. For some nodes however, a different minimum service pressure exists due to the nature of the connected customer. For example, the minimum pressure constraint at the CP of DMA 2 (Figure 2) has been set to $21mH_2O$ due to the presence of a tall building. The DMAs also supply critical customers including two hospitals and a large industrial user. Before the installation of the dynamic DMA topology, these DMAs were identified as having a

high AZP and little security of supply for the critical users (hospitals) because only one supply route is available for each of the single-feed DMAs.

The installation of the dynamic DMA topology included the replacement of two closed boundary valves with dynamic boundary valves (DBV 1 and DBV 2, as shown in Figure 2), and the retrofitting of two PRVs (PRV 1 and PRV 2) with the same technology, which was outlined in Section 2.1. An additional 21 sensors that measure pressure at a frequency of 128S/s (InfraSense TS) are placed throughout the WDN to provide key measurements that aid in the calculation of AZP as well as additional information about the control efficiency and other events. At control valve sites where power is available, data is communicated in real-time via an ADSL link installed in a nearby kiosk as shown in Figure 3 and offers instantaneous visibility of the network status. Flow measurements are also transmitted in real-time and are used to assess the network behaviour and update demand usage patterns in the hydraulic model.

In this paper, the AZP of two configurations of DMA operation are investigated through the experimental programme: a static DMA topology (closed boundary valves) and a dynamic DMA topology where the DBVs are programmed to open during the day, and close at night for leakage detection activities. The calculation and actuation of optimal valve settings for PRV 1 and PRV 2 (Figure 2) in both configurations is undertaken using a novel optimization method based on strictly feasible sequential convex programming, as outlined in the following section.

3. Control Optimization

To determine optimal PRV settings in the experimental programme, a mathematical optimization problem (that employs the steady-state hydraulic system behavior as a set of

nonlinear constraints) is solved. A number of optimization methods have been proposed for this purpose and are summarized in Section 3.2. The optimization problem is solved multiple times to reflect hydraulic changes (i.e. customer demands, reservoir levels) in the WDN. Open-loop PRV settings can therefore be constructed. The implementation of these open-loop PRV settings is discussed in section 4.1.

3.1. Problem Formulation

We consider a demand-driven model for a WDN, which is represented by a graph consisting a set of nodes N_n, where $|N_n| = n_n$, a set of reservoirs N_o, where $|N_o| = n_o$, a set of links N_p, where $|N_p| = n_p$, and a set of PRVs N_v, where $|N_v| = n_v$ and $N_v \subseteq N_p$. The mass and energy conservation laws that describe the WDN are defined by the set of equations:

$$g_1(q, h, \eta; h_0) := A_{11}(q)q + A_{12}h + A_{10}h_0 + A_{13}\eta = 0, \tag{1}$$

$$g_2(q; d) := A_{12}^T q - d = 0, \tag{2}$$

where $h \in \mathbb{R}^{n_n}$ are the nodal piezometric heads, $q \in \mathbb{R}^{n_p}$ are the pipe flows, $\eta \in \mathbb{R}^{n_v}$ are the PRV settings, the matrices $A_{12} \in \mathbb{R}^{n_p \times n_n}$, $A_{13} \in \mathbb{R}^{n_p \times n_v}$, and $A_{10} \in \mathbb{R}^{n_p \times n_o}$ are incidence matrices describing the relationship between links and nodes, valves and reservoirs respectively. The variable $d \in \mathbb{R}^{n_n}$ represents water demand at nodes (assumed known), $h_0 \in \mathbb{R}^{n_o}$ are known heads. The square matrix $A_{11} \in \mathbb{R}^{n_p \times n_p}$ is a diagonal matrix with the elements

$$A_{11}(i, i) = r_i |q_i|^{n_i - 1}, i = 1, \ldots, n_p, \tag{3}$$

where $r \in \mathbb{R}^{n_p}$ is the vector of frictional resistance factors of the pipes and $n \in \mathbb{R}^{n_p}$ are constants related to the frictional head loss. In this article, the Hazen-Williams friction

formula is used to model frictional losses; $n_i = 1.85$ and $r_i = \frac{10.675 L_i}{c_i^{n_i} D_i^{4.87}}$, where L_i, D_i and c_i denote the length, diameter and roughness coefficient of pipe i, respectively. For valves, $n_i = 2$ and an empirical value for r_i is generally supplied by the valve manufacturer.

To find the optimal PRV settings that minimize the AZP of the WDN, we solve the optimization problem:

$$\min_{\eta,q,h} f(h;\eta,q) := \sum_{j=1}^{n_n} \omega_j h_j, \tag{4a}$$

$$\text{subject to: } g_1(\cdot) = 0 \tag{4b}$$

$$g_2(\cdot) = 0 \tag{4c}$$

$$-q_i \leq 0, \ \forall i \in N_v \tag{4d}$$

$$-\eta_i \leq 0, \ \forall i \in N_v \tag{4e}$$

$$\underline{h}_j - h_j \leq 0, \ \forall j \in N_n \tag{4f}$$

where $g_1(\cdot)$ and $g_2(\cdot)$ are the conservation equations (1) and (2), respectively, and the inequality constraints (4f) come from the need to satisfy the minimum service level guarantees. The component-wise positive constants in $\underline{h} \in \mathbb{R}^{n_n}$ are the minimum service level heads for each node. The inequality constraints (4d) and (4e) come from the physical constraint that PRVs regulate pressure in a single direction. The coefficients $\omega \in \mathbb{R}^{n_n}$ in (4a) relate the AZP to the nodal pressures by weighting each node by the length of its incident links. That is,

$$\omega_j = \bar{L}^{-1} \sum_{i \in \mathcal{I}_j} \frac{L_i}{2}, \qquad \bar{L} = \sum_{i=1}^{n_p} L_i, \tag{5}$$

where $\mathcal{I}_j$ is the set of indices for links incident at node j and L_i is the length of the i^{th} pipe.

In the optimization problem (4), PRVs are modelled using the linear term η, which represents the additional head loss within links containing a PRV. Therefore, if for PRV i, $\eta_i = 0$, the PRV is fully open, and the total head differential is equal a minor loss represented by $r_i q_i^{n_i}$ for the valve. Although (4) has a linear objective (4a) and linear inequality constraints(4d)–(4f), the equality constraint for energy conservation (4b) is nonlinear due to the nonlinear frictional loss terms of the form $r_i q_i |q_i|^{n_i - 1}$. This results in a nonlinear program (NLP) that is also non-convex, since flow in pipes is bi-directional. In addition, the use of the Hazen-Williams head loss formula means the problem is non smooth at flows $q_i = 0$. Although generic NLP solvers can be used to solve (4), greater computational efficiency and reliability of solutions can be achieved if the problem structure is taken into account [*Wright et al.*, 2014]. This is particularly important when implementing real-time control and so is our approach in this article.

3.2. Review of valve optimization

Optimization of valve control has generally been studied with the intention of reducing either pressure or leakage in WDNs. *Jowitt and Xu* [1990] used a sequential linear programming (SLP) method to minimize leakage for a small example network consisting of 25 nodes. *Vairavamoorthy and Lumbers* [1998] used the same network to demonstrate a sequential quadratic programming (SQP) method. In addition, an objective function that minimizes the difference between target and actual nodal pressure was investigated, which allows minor pressure violations at nodes in order to achieve a larger overall reduction in network pressure. *Ulanicki et al.* [2000] solved an NLP for reducing leakage in simulation by using a commercial NLP solver. In addition, each optimized valve profile was correlated with the valve's flow to produce a control curve (also called a flow modu-

lation curve), an approach that is used in this paper to actuate control (Section 4.1). For large networks, *Ulanicki et al.* [2000] used the model skeletonization technique proposed by *Ulanicki et al.* [1996] to reduce the computation time. *Skworcow et al.* [2010] used the same NLP solver for the combined optimization of PRVs and pumps on a skeletonized network. They proposed model predictive control (MPC) for the control implementation. MPC involves the periodic finite-time optimization of the future state of the WDN model and the calculation and implementation of optimal valve settings based on this future horizon. Due to limitations in telecommunications, the MPC approach was only used in simulation.

The simultaneous optimization of valve placement and valve settings was considered in (*Eck and Mevissen* [2013], *Eck and Mevissen* [2012]). A key aspect of their implementation was the approximation of the Hazen-Williams relationship by quadratic function. Two variables representing flows in opposite directions were assigned to each pipe but with a complementarity condition that at least one of the flows is zero. This approach therefore avoids the discontinuity at $q_i = 0$ when using the Hazen-Williams head loss formula. Two case studies were used: the small illustrative network from *Jowitt and Xu* [1990] and a larger network ('Exnet') consisting of approximately 1,900 nodes introduced to the research community as a more realistic WDN model by *Farmani et al.* [2004]. The quadratic approximation resulted in a pressure and flow solution that generally agreed well with hydraulic simulation solutions from EPANET although some reported errors were as high as 0.75l/s. The recorded solution time for optimizing the settings of 4 control valves (fixed valve placements) in 'Exnet' was 121 seconds. *Nicolini and Zovatto* [2009] also solved a combined valve placement and control problem using genetic algorithms (GA),

which are particularly useful when multiple objective functions are evaluated. Whilst heuristics such as GA are highly applicable to design problems and often find good solutions in the search space, they generally require high computation times due to the large number of hydraulic simulations involved in finding a good solution and are not generally appropriate for near real-time control applications.

For the optimization method used for PRV control in our experimental programme, a number of strict criteria were set out that have not all been addressed by previous work in the literature. The criteria are as follows:

- Reliable convergence: An optimization method used in near real-time control must be able to perform under a wide range of hydraulic conditions and produce a control solution consistently.
- Rapid convergence: The optimization should also be computationally cheap to carry out. This ensures that valve settings can be calculated rapidly when hydraulic changes occur in the network. It also facilitates the optimization to be run on less powerful computers or servers, making it accessible to more users.
- An exact representation of the hydraulic model without simplification or skeletonization. This ensures as much accuracy is retained as possible in the control solution and also aids in the scalability of the solution method to bigger networks or different objective functions.

An optimization method based on SCP was proposed in [*Wright et al.*, 2014] that addressed the above criteria. An SCP method solves a non-convex NLP problem by sequentially solving convex approximations (sub-problems). The convexity of each approximation means each sub-problem can be solved accurately and efficiently. SCP methods

differ from other sequential optimisation methods (SLP, SQP) because they preserve convexity in the problem, even if this convexity is non-linear [*Dinh et al.*, 2011]. SCP was used by [*Quoc et al.*, 2012] to successfully solve near real-time control problems. Its major advantage is that it can generally converges well to a feasible point with a good or optimal objective function value. In [*Wright et al.*, 2014], the SCP method was applied to a PRV control problem and showed good convergence properties under various different hydraulic conditions. In this paper, we are interested in controlling PRVs and DBVs. The introduction of DBVs that follows a position controlled schedule (i.e. open in the day, closed at night) resulted in the SCP method from [*Wright et al.*, 2014] occasionally getting stuck outside the feasible optimization search space. In this paper, we improve the convergence of the SCP method by guaranteeing that each step in the optimization is strictly feasible.

3.3. Strictly Feasible Sequential Convex Programming for Valve Optimization

Let the optimization variables and the equality constraints of (4b)–(4c) be reformulated as $x := [q^T\ h^T\ \eta^T]^T$ and $g(x) := [g_1(x)^T\ g_2(x)^T]^T \in \mathbb{R}^{n_p+n_n}$, respectively. We define the hydraulic feasibility region by the set

$$\mathbb{E} := \{x \in \mathbb{R}^{n_p+n_n+n_v} : x \text{ satisfies (4b), (4c), (4d), and (4e)}\}. \tag{6}$$

Similarly, the inequality feasibility region for the PRV setting and performance constraints is defined by the set

$$\mathbb{F} := \{x \in \mathbb{R}^{n_p+n_n+n_v} : x \text{ satisfies (4d), (4e) and (4f)}\}. \tag{7}$$

When the SCP framework [*Quoc et al.*, 2012] is applied to (4) for given parameters d and h_0, the algorithm structure is as follows:

Step 1. Choose a hydraulically feasible $x^1 \in \mathbb{E}$, Set $k = 1$

Step 2. To get the new iterate x^{k+1}, solve the convex subproblem:

$$\min_x \ c^T x \tag{8a}$$

subject to:

$$g'(x^k)(x - x^k) + g(x^k) = 0, \tag{8b}$$

$$x \in \mathbb{F} \tag{8c}$$

where the coefficient vector c contains the vector of weights w_i and $g'(x)$ is the Jacobian of the constraint matrix g.

Step 3. STOP IF stopping criteria is satisfied. ELSE, set k to $k + 1$ and Go back to Step 2.

The subproblem (8) is formed by linearizing the equality constraints, specifically (4b). The equality constraint (8b) has the expression

$$NA_{11}(q^k)(q - q^k) + A_{11}(q^k)q^k + A_{12}h +$$

$$A_{10}h_0 + A_{13}\eta = 0, \tag{9a}$$

$$A_{12}^T q - d = 0, \tag{9b}$$

in terms of the flows, heads and PRV settings, where $N = \texttt{diag}(n_i),\ i = 1, \ldots, n_p$. With x^k being a known constant at the current iteration k, the constraints (9) are all linear in the unknown x. Therefore, the resulting optimization problem (8) has a linear objective and linear equality and inequality constraints; it is, therefore, a convex program and can be solved efficiently [*Luenberger and Ye*, 2008]. This makes the SCP approach even more attractive since state-of-the art interior-point solvers can be used even for large scale linear programs, where the sparsity structures in the constraints are taken advantage of *Nocedal and Wright* [2006].

In [*Wright et al.*, 2014], this SCP framework was investigated. Although the iterates x^{k+1} that solve (8) satisfy the linear equality constraint(4c), they would not satisfy the nonlinear equality (4b) and so would not be hydraulically feasible. In principle, these iterates can be projected onto the intersection of hydraulic feasibility and performance inequality constraint sets $\mathbb{E} \cap \mathbb{F}$. Even for convex nonlinear constraint sets, the substantial overhead associated with projected methods is a main drawback [*Bertsekas*, 1999, Sec. 2.3]. Since the effort of projecting the solution $x^{k+1} \in \mathbb{F}$ onto the intersection of the linear and nonlinear constraint sets can be as complicated as solving the original optimization problem, an approximate approach to projection was used in [*Wright et al.*, 2014] to maintain hydraulic feasibility at each step.

The method starts by solving a hydraulic equation, where the PRVs are set to fully open for the first iteration. With the PRV setting $\eta^1 = 0$, (1) and (2) are solved to find q^1 and h^1 such that $x^1 \in \mathbb{E}$. After Step 2 of each iteration k, the value η^{k+1} from the solution $x^{k+1} \in \mathbb{F}$ of (8) was fixed as the PRV setting and a hydraulic solver was used to find another $\hat{q}^{k+1}$ and $\hat{h}^{k+1}$ that satisfy (1) and (2) for this PRV setting; i.e. a 'sort of projection' of x^{k+1} onto the hydraulic feasibility set $\mathbb{E}$ is used to guarantee the hydraulic conservation equations are satisfied. A 'sort of projection' because the updated values $\hat{q}^{k+1}$ and $\hat{h}^{k+1}$ may not satisfy the performance constraints, i.e. $\hat{x}^{k+1} = [\hat{q}^{k+1};\ \hat{h}^{k+1};\ \eta^{k+1}]$ may not be in $\mathbb{F}$. Setting k to $k+1$, the linearized convex problem in Step 2 was then solved with $\hat{x}^{k+1}$. This process was repeated until the objective function evaluated for $x^k \in \mathbb{E}$ decreased sufficiently and the difference between the linear program solution and its 'projection' onto the hydraulic feasibility set $\mathbb{E}$, i.e. $\|x^{k+1} - \hat{x}^{k+1}\|$, was within a specified small tolerance.

It was shown in [*Wright et al.*, 2014] that this approach worked well most of the time. However, the method sometimes failed to converge to a feasible solution for the original optimization problem (4). For example, η^{k+1} computed at Step 2 would sometimes result in a solution that violates (4f) when projected onto $\mathbb{E}$, which occasionally led to convergence difficulties. One example of this is shown in Figure 4a. Here, the SCP method from [*Wright et al.*, 2014] is applied to the case study in Figure 2. The contours represent the objective function when two PRVs are operational and the shaded region represents the feasible region $\mathbb{E} \cap \mathbb{F}$, i.e. the space where the constraints (4b) – (4f) are all satisfied. The optimization method takes steps outside of the feasibility region initially, and eventually oscillates in an infeasible search space for the original optimization problem (4). This either resulted in an infeasible solution after the maximum number of iterations or in sub-optimality when the final solution was 'projected' onto the feasibility region.

In this article, we propose the use of strictly feasible iterates to stabilize the algorithm and to achieve convergence. In the spirit of feasible direction descent methods [*Bertsekas*, 1999, Sec 2.2], we generate a sequence of feasible iterates by using line searches along descent directions; in our strictly feasible SCP, a simple line search is used to guarantee a descent in the objective function and feasibility at each iteration, which together guarantee convergence to a local minima. The SFSCP algorithm can only guarantee convergence to locally optimal solutions because the original problem is nonconvex. Although it is generally not possible to show a linear or better rate of convergence for SCP methods, we do not attempt to prove convergence properties as it is beyond the scope of this paper. SCP methods can also sometimes have slow convergence very near to solutions [*Schittkowski and Zillober*, 2005]. Nonetheless, SCP methods are generally known to have fast

convergence to optimal points in many practical optimization problems [*Ni et al.*, 2005]. As will be shown in Section 4.1, this is the case in our optimization problem.

For a given feasible iterate x^k, a feasible direction at x^k is a non-zero vector d^k that guarantees $x^k + \alpha d^k$ is feasible for all $\alpha \in (0, \theta]$ with some $\theta > 0$ that is sufficiently small. From Figure 4a, we note that the first iterate of the SCP is taken along a feasible descent direction. Since the descent direction is one that reduces pressure heads, taking a full-step in this direction can violate the minimum pressure constraints (4f). Moreover, if the feasible iterate is on the boundary of the feasibility space $\mathbb{E} \cap \mathbb{F}$, where the constraints (4f) are active, the descent directions may not even be feasible. Like feasible interior point methods [*Nocedal and Wright*, 2006], we propose making our iterates strictly feasible by approaching the boundary of $\mathbb{E} \cap \mathbb{F}$ from the interior of the constraints (4f). Unlike interior point methods we do not use barrier function but rather enforce strict feasibility in the 'projection' stage of our SCP approach.

In this new approach, the valve settings η^{k+1}, which are computed by solving the linear program in Step 2 of the k^{th} iteration in SCP algorithm, are not used directly to find a 'projection'/solution in $\mathbb{E}$ via hydraulic simulations. Instead, η^{k+1} is used to form a feasible descent direction, and a line search is performed to find a next iteration that is guaranteed to be both feasible and lower in objective function value.

3.4. Line Search

Line search methods are used in optimization to determine step sizes that minimize or decrease the objective function $f(\cdot)$ along a search direction. With the search direction

defined as

$$d\eta^k = \eta^{k+1} - \eta^k, \tag{10}$$

we use a line search to find a step-size α^k that guarantees a reduction in objective function value by evaluating:

$$f(q^{k+1}, h^{k+1}, \eta^k + \alpha d\eta^k) = \sum_{j=1}^{n_n} \omega_j h_j^{k+1} \tag{11}$$

and checking that the next iterate x^{k+1} is strictly feasible with respect to all the constraints, i.e. $x^{k+1} \in \mathbb{E} \cap \mathbb{F}$. Since it is not always possible to find a feasible descent direction from an iterate on the boundary of the feasible set, we want to restrict initial iterations of the optimization from getting too close to the infeasible space – the iterates will be in the interior of the feasible region at all iterations of a strictly feasible optimization method. In order to discourage initial iterations from becoming close to the infeasible space, $\epsilon -$ feasibility is enforced. At the k^{th} iteration of the SCP, the line search considers feasibility that is $\epsilon(k)$ of (4f) as follows:

$$\underline{h}_j - h_j + \epsilon(k) \leq 0, \ \forall j \in N_n, \ \epsilon(k) > 0 \tag{12}$$

where $\epsilon(k)$ decreases with SCP iteration number as

$$\epsilon(k) = \frac{1}{k^2}. \tag{13}$$

As can be seen from (13), $\epsilon(k) \to 0$ as k increases. Therefore, the inequality (12) becomes arbitrarily close to (4f) as we approach a local optimum on the boundary. It is also clear that an x^{k+1} that satisfies (4b), (4c), (4d), (4e) and (12), is also in the set $E \cap \mathbb{F}$.

The type of line search used in this paper is partly inspired by the Armijo rule from the Wolfe conditions and Backtracking line search principles. An Armijo method enforces a

'sufficient' decrease in the objective along the descent direction [*Bertsekas*, 1999]. Since a full step will not necessarily maintain strict feasibility of all constraints, we instead only require that $f(\cdot)$ decreases at each iteration. For practical purposes this works well, since $f(\cdot)$ decreases rapidly along the search directions $d\eta^k$ as seen in Figure 4b, and quickly gets very close to a local minimum.

In Backtracking line searches, initially the full step is taken (i.e. $\alpha = 1$) and subsequently reduced until a stopping condition is satisfied [*Boyd and Vandenberghe*, 2004]. The same principle is used in this paper by first taking a unit step ($\alpha = 1$) and updating α subsequently until the line search stopping criteria are satisfied. The stopping criteria is that the next iterate is feasible ($\mathbb{E} \cap \mathbb{F}$) and that it has a lower objective function value.

The line search is carried out using a two step process as follows. For the first iteration of the line search, $\alpha = 1$ and

1. Compute $f(\cdot, \eta^k + \alpha d\eta^{k+1})$
2. IF $f(\cdot, \eta^k + \alpha d\eta^k) < f(\cdot, \eta^k)$ AND the next iterate is feasible, then $\eta^{k+1} = \eta^k + \alpha d\eta^k$

   ELSE set $\alpha = \alpha/2$, return to return to step 1

For the example shown in Figure 4a, this process of ensuring iterations are strictly feasible is shown in Figure 4b. Here it is guaranteed that each step both decreases $f(\cdot)$ and is strictly inside the feasible set $\mathbb{E} \cap \mathbb{F}$ shown by the shaded area. In the latter iterations of the optimization, allowing the ϵ^k to become sufficiently small enables the solutions to get arbitrarily close to the local optima. Moreover, a practical stopping criteria that the relative decrease in the objective function is within some tolerance λ_{tol} is used here, i.e. termination is triggered when $\frac{f^k - f^{k+1}}{f^k} < \lambda_{tol}$. In our examples, we found that a value of

449 10^{-3} for λ_{tol} was sufficiently small. Our SFSCP method is summarised in Algorithm 1,
450 where we denote a hydraulic simulation that solves (1) and (2) by HS.

3.5. Hydraulic analysis for equality constraints

451 In [*Wright et al.*, 2014], (1) and (2) was solved only once at each iteration of the opti-
452 mization method. The solution was calculated using a Newton method initially proposed
453 by *Todini and Pilati* [1988] and commonly referred to as the nodal Newton-Raphson
454 method. In this paper, the solution to (1) and (2) is calculated at least twice for each
455 iteration of the optimization method. When calculating PRV settings for extended period
456 simulations, this can lead to a large increase in computing time. The solution to (1) and
457 (2) represents the most computationally intensive part of our optimization method. We
458 therefore require an efficient method for the hydraulic analysis problem. In [*Abraham and*
459 *Stoianov*, 2015], a null space algorithm for hydraulic analysis is shown to have superior
460 computational efficiency for hydraulic analysis of sparse networks. The structure of the
461 system of equations in (1) and (2) is that of a saddle point system, which null space
462 algorithms take advantage of. The method starts with an initial solution to (2) by using,
463 for example, a least square method. A null space basis is then generated and further
464 Newton iterations are carried out in this space until (1) is also satisfied. The method
465 offers strong improvements in computational speed particularly when $n_p - n_n$ is small,
466 which is generally the case for most real networks [*Elhay et al.*, 2014]. In [*Abraham and*
467 *Stoianov*, 2015], further computational efficiency is achieved by carrying out updates of
468 headlosses at each Newton iteration only for links whose flows have not yet converged.

469 Another advantage of using the null space algorithm is its ability to handle links with
470 a zero flow. Typically, methods such as the nodal Newton scheme do not accurately

calculate zero flows, which can result in poor convergence when used in optimization problems. This is because when $q_i = 0$, $A_{11}^{-1}(q)$ becomes singular when using the Hazen-Williams head loss formula. The optimization of WDNs with a dynamic topology will always have zero flows because the boundary valves generally close at night resulting in a zero flow between interconnected DMAs. In the null space approach, no such matrix inversion is required. Moreover, by using a Jacobian regularization within the null space algorithm, it is possible to avoid ill-conditioning of the linear systems of the Newton method.

Data: Network structure, configuration and hydraulic data (A_{12}, A_{10}, A_{13}, H_0, d)
Result: Valve settings (η)
Initialization: Set $\eta = 0$, $k = 1$;
h^k, $q^k \longleftarrow HS(\eta^k)$;
while $f^k - f^{k+1} > \lambda_{tol}$ **and** $k \leq k_{max}$ **do**
  $\eta^{k+1} \longleftarrow$ solution to (8) ;
  $d\eta^k \longleftarrow \eta^{k+1} - \eta^k$;
  Set $\alpha = 1$;
  h^{k+1}, $q^{k+1} \longleftarrow HS(\eta^k + \alpha d\eta^k)$;
  while $f^{k+1} > f^k$ **or** $x^{k+1} \notin \mathbb{E} \cap \mathbb{F}$ **do**
    $\alpha \longleftarrow \alpha/2$;
    h^{k+1}, $q^{k+1} \longleftarrow HS(\eta^k + \alpha d\eta^k)$;
  end
  $\eta^{k+1} \longleftarrow \eta^k + \alpha d\eta^k$;
  $k \longleftarrow k + 1$
end

Algorithm 1: SFSCP

4. Results and Discussion

4.1. Optimization Results

The SFSCP algorithm outlined in the previous section was used to calculate open-loop pressure profiles for PRV 1 and PRV 2 in the experimental programme shown in Figure 2 for both a closed DMA topology and a dynamic DMA topology. In all simulations, SFSCP successfully converged to a local optimal control solution, with an average of 9 iterations required to meet the convergence criterion.

This section only details the implementation of the optimized PRV settings in the dynamic DMA topology configuration. The implementation of the PRV settings for the closed DMA configuration follows the same procedure, with the exception that the boundary valves are fully closed at all times. The comparison of AZP are then shown for both a dynamic and closed DMA topology.

The optimized PRV outlet pressure profiles are shown in Figure 5a and Figure 5b. It is observed that each PRV outlet pressure is correlative to the PRV flow, therefore it is possible to establish and implement a flow modulation curve, i.e. a relationship between outlet pressure and flow. This facilitates near optimal valve settings to be actuated locally on each PRV using local flow measurements captured with a flow meter. Flow modulation is an emerging form of advanced pressure management. There are many suppliers of the technology [*Technolog*, 2014; *i2O*, 2014; *Palmer*, 2015] and consequently flow modulation is becoming increasingly implemented in industry. More information on flow modulation and other PRV control approaches is reviewed by *Ulanicki et al.* [2000] and *Wright et al.* [2014].

The flow modulation curves constructed are shown in Figure 6. It is observed that the range in outlet pressure of each flow modulation curve is proportionate to the distance between the PRV and its nearest CP as shown in Figure 2. More specifically, there is a large distance between PRV 1 and the CP of DMA 1 and only a small distance between PRV 2 and the CP of DMA 2. A larger distance between the PRV and CP results in larger frictional head losses and a need to provide a higher outlet pressure to maintain pressure above the minimum threshold. It is seen that the fitted flow modulation curve for PRV 1 has a much wider range of outlet pressures than the flow modulation curve for PRV 2, which demonstrates that the PRVs each control a separate critical point under these particular hydraulic conditions when the objective is the minimization of AZP.

The hydraulic simulation results for the boundary valves are shown in Figure 5c and Figure 5d. In the hydraulic model and optimization, the boundary valve open to 20% during the day and close fully at night (i.e. 20% open 07:00 - 00:30 and fully shut 02:30 - 05:30). During the hours 00:30 - 02:30 and 05:30 - 07:00, the boundary valves are incrementally closing and opening respectively. In order to avoid undesirable pressure transients and achieve a stable operation, the boundary valves open/close slowly over a period of approximately two hours. The boundary valve schedule was provided by the DMA managers and facilitates their leakage assessments using the minimum night flow. It is seen in Figure 5c and Figure 5d that the DBVs provide a route for water between the two DMAs. At night the DBVs close down automatically and the flow between DMAs reduces to zero. The minimum night flow can then be accurately measured and leakage estimations made.

4.2. Experimental Programme Implementation

PRV 1 and PRV 2 are uploaded with the flow modulation curves shown in Figure 6 and the DBVs follow the opening schedule defined in section 4.1. The experimental programme network is monitored using the real time data and analyzed for the following:

- Actuation of control: It is important to ensure that the optimized valve settings have been actuated correctly at the PRVs. This is undertaken by analyzing the data at the PRVs and comparing this with the flow modulation curve. For example, Figure 7 shows the hydraulic data for PRV 1 and the flow modulation curve derived from the optimization that it follows. The PRV successfully follows the curve with an R^2 value of 0.94.
- Model and data comparison: This involves the comparison of the model pressure at nodes where data is available. For example, Figure 8 shows the pressure at CP 1 (Figure 2) according to the hydraulic model (simulated with both the optimal open-loop PRV settings and the fitted flow modulation curves defined in Figure 6 for PRV 1 and PRV 2), and pressure data from a remote logger deployed at CP 1 (data plotted at 5 samples/s). The pressure at CP 1 according to the hydraulic model when optimal open-loop valve settings are used at the PRVs is exactly $15mH_2O$, which represents the minimum allowable pressure. This is to be expected, since the objective function was to minimize AZP subject to a minimum allowable pressure. By using the optimal outlet pressure profiles in the hydraulic model, this target pressure is achieved at the CP. When the flow modulation curves are used for PRV 1 and PRV 2 in the hydraulic model, pressure at CP 1 remains close to $15mH_2O$ but fluctuates above and below this value. This is because there are some small discrepancies between the flow modulation curve and the optimal valve set point (Figure 6). Finally, the hydraulic data also shows that pressure at the CP is also

fluctuating above and below CP 1. A minimum pressure value of $13.27mH_2O$ occurs. Discrepancies here are due to the stochastic nature of customer demand, uncertainty in the hydraulic model, and the discrepancies between the optimal PRV set point and the flow modulation curve. The data shows that the PRV control has successfully controlled pressure such that the CP is close to $15mH_2O$. This methodology for checking the valve actuation and network behaviour is repeated for other points of the WDN to further validate the optimization method, hydraulic model and control. As recommended by [*Committee et al.*, 1999], pressure measurements are within $\pm 2mH_2O$ of the steady state hydraulic model for 100% of the logged nodes.

In order to assess the AZP benefits of operating a dynamic DMA topology over a closed, static DMA topology, the experimental programme is operated consequently using the two configurations outlined above, each for a 5 day period. The first configuration has a dynamic topology (where BV1 and BV2 open to 20% each day) and the flow modulation curves shown in Figure 6 controlling PRV 1 and PRV 2. The second configuration has a closed DMA topology (i.e. BV1 and BV2 set to 100% closed at all times) and optimized flow modulation curves configured on the PRV 1 and PRV 2 that were calculated using the SFSCP methodology. The total WDN water input is then measured using the flow meters and the results are shown in Figure 9. It is observed that over the 5 day period, approximately 1 million less litres are used in the DMAs of the experimental programme when a dynamic topology is in operation, which is a reduction of approximately 5%. A reduction in AZP of 2.8% was also observed using the hydraulic model. Although the length of this case study is limited, it shows that a dynamic topology provides promising results for the reduction of AZP and leakage. Based on the modelling and the SFSCP

optimization method alone, AZP reductions of up to 6.5% can be achieved when opening the boundary valves fully to 100% as shown in Figure 10.

5. Conclusion

Water companies are becoming increasingly committed to improving customer service levels and further reduce leakage. Whilst fixed topology DMAs have helped them to identify leakage hotspots, a permanent reduction in network redundancy has resulted in reduced resilience to failure, suboptimal pressure management, and water quality concerns. Operating a dynamic DMA topology is a novel approach towards leakage and pressure management that can address these drawbacks whilst still retaining the success in identifying and reducing leakage that fixed topology DMAs have facilitated.

The novel contributions of this paper can be summarised as follows:

- The optimal control of a WDN with dynamic DMA topology is a valve control problem. Since the dynamic aggregation of DMAs can result in very large and complex network models forming, convergence problems can be caused that are not present when smaller, more simple networks are optimized. This paper addresses these convergence problems by developing a novel optimization algorithm based on strictly feasible sequential convex programming that minimizes AZP. By guaranteeing feasibility at each iteration step, reliable convergence could be achieved. The method made use of a null space hydraulic algorithm to improve computational efficiency.
- The optimized valve control was successfully actuated in a real, operational WDN operating with a dynamic DMA topology. This unique experimental programme demonstrated the successful implementation of the novel dynamic DMA topology concept.

589 • A reduction in AZP of 2.8% was observed experimentally when operating a dynamic DMA
590 topology over a closed, static DMA topology. Over a 5 day period, a 5% reduction in
591 DMA water input was observed, equivalent to 1Ml of water. It is estimated in simulation
592 that opening the boundary valves to 100% will result in an AZP reduction of 6.5%.

593 Further analytical and experimental research is required in control optimization, mod-
594 elling and water quality analysis in order to fully identify the benefits and challenges
595 associated with the operation of DMAs with a dynamic topology. This should focus on:

596 • Long term studies to compare the pressure management of a dynamic topology in com-
597 parison to other operational approaches, including a static DMA structure.

598 • The exploration of other control strategies for the dynamic topology. In this paper, flow
599 modulation curves were produced and the DBVs were programmed with an open-loop
600 schedule that allows water companies to utilize added redundancy during the day, and
601 carry out leakage management at night. Other control strategies include model predictive
602 control for the optimal control of PRVs and DBVs. Valve control in failure scenarios is
603 also an unexplored research area.

604 • An investigation into the other benefits of operating a dynamic DMA topology, such
605 as water quality and resilience improvements. The resilience investigation can include
606 resilience assessments using both hydraulic measures and graph theoretic approaches.

607 • An investigation into the cost-benefit ratio of the proposed dynamic DMA topology con-
608 cept. The requirement for additional equipment for the operation of a dynamic DMA
609 topology increases installation and maintenance costs over standard DMA control prac-
610 tices. An investigation into the cost savings made from improved network resilience and

pressure management needs to be undertaken in order to justify the investment and scalability of a dynamic DMA topology.

Acknowledgments. The authors are grateful for the financial support and technical expertise of Bristol Water plc and Cla-Val Ltd. The authors also acknowledge the funding supplied by the Engineering and Physical Sciences Research Council. The second author is supported by the NEC-Imperial "Big Data Technologies for Smart Water Networks" project. More details on algorithm implementation or data can be made available to the interested readers by emailing the authors.

References

Abraham, E., and I. Stoianov (2015), Sparse null space algothims for hydraulica analysis of large scale water supply networks, *Journal of Hydraulic Engineering*, *11*(1), 1111–1111.

Armand, H., I. Stoianov, and N. Graham (2015), Investigating the impact of sectorized networks on discoloration, *Procedia Engineering*, *119*, 407–415.

Bertsekas, D. (1999), *Nonlinear Programming*, second ed., Athena Scientific.

Boyd, S., and L. Vandenberghe (2004), *Convex optimization*, Cambridge university press.

Cla-Val (2015a), D22 pilot controller for position, pressure, flow, and modulation control, [Online; accessed 20-04-2015].

Cla-Val (2015b), e-flowmeter for flow measurements based on the vortex shedding phenomenon, [Online; accessed 20-04-2015].

Cla-Val (2015c), e-power mp for energy harvesting, [Online; accessed 20-04-2015].

Committee, A. E. C. A., et al. (1999), Calibration guidelines for water distribution system modeling, in *Proceedings of the 1999 AWWA Information Management and Technology*

Conference (IMTech), New Orleans, Louisiana.

Dinh, Q. T., C. Savorgnan, and M. Diehl (2011), Real-time sequential convex programming for nonlinear model predictive control and application to a hydro-power plant, in *Decision and Control and European Control Conference (CDC-ECC), 2011 50th IEEE Conference on*, pp. 5905–5910, IEEE.

Drinking Water Inspectorate (2009), Drinking water safety: Guidance to health and water professionals.

Eck, B. J., and M. Mevissen (2012), Valve placement in water networks: Mixed-integer non-linear optimization with quadratic pipe friction, in *Company Report*.

Eck, B. J., and M. Mevissen (2013), Fast non-linear optimization for design problems on water networks, in *World Environmental and Water Resources Congress 2013*.

Elhay, S., A. R. Simpson, J. Deuerlein, B. Alexander, and W. H. Schilders (2014), Reformulated co-tree flows method competitive with the global gradient algorithm for solving water distribution system equations, *Journal of Water Resources Planning and Management*, *140*(12).

Fantozzi, M., F. Calza, and A. Lambert (2009), Experience and results achieved in introducing district metered areas (dma) and pressure management areas (pma) at enia utility (italy), in *IWA International Specialised Conference Water Loss*.

Farmani, R., D. A. Savic, and G. A. Walters (2004), Exnet benchmark problem for multiobjective optimization of large water systems, *Modelling and Control for Participatory Planning and Managing Water Systems*.

Hoskins, A., and I. Stoianov (2014), Infrasense: A distributed system for the continuous analysis of hydraulic transients, *Procedia Engineering*, *70*, 823–832.

i2O (2014), Advanced pressure management, [Online; accessed 05-06-2014].

Jowitt, P. W., and C. Xu (1990), Optimal valve control in water-distribution networks, *Journal of Water Resources Planning and Management*, *116*(4), 455–472.

Lalonde, A., C. Au, P. Fanner, and J. Lei (2008), City of toronto water loss study and pressure management pilot, *Miya Arison Group, unpublished*.

Luenberger, D. G., and Y. Ye (2008), *Linear and nonlinear programming*, vol. 116, Springer Science & Business Media.

Ni, Q., C. Zillober, and K. Schittkowski (2005), Sequential convex programming methods for solving large topology optimization problems: implementation and computational results, *Journal of Computational Mathematics -International Edition-*, *23*(5), 491.

Nicolini, M., and L. Zovatto (2009), Optimal location and control of pressure reducing valves in water networks, *Journal of water resources planning and management*, *135*(3), 178–187.

Nocedal, J., and S. J. Wright (2006), *Numerical optimization*, Springer Verlag.

Ofwat (2007), Security of supply 2006-07 report, [Online; accessed 05-06-2014].

Ofwat (2008), The guaranteed standards scheme (gss), [Online; accessed 15-03-2015].

Ofwat (2012), The service incentive mechanism (sim), [Online; accessed 05-06-2014].

Ofwat (2014), Setting price controls for 2015-20 pre-qualification decisions, [Online; accessed 23-04-2015].

Palmer (2015), Pressure control, [Online; accessed 15-03-2015].

Piller, O., B. Bremond, and M. Poulton (2003), Least action principles appropriate to pressure driven models of pipe networks, in *ASCE Conf. Proc. 113*, pp. 19–30.

Quoc, T. D., C. Savorgnan, and M. Diehl (2012), Real-time sequential convex programming for optimal control applications, in *Modeling, Simulation and Optimization of Complex Processes*, pp. 91–102, Springer.

Schittkowski, K., and C. Zillober (2005), Sqp versus scp methods for nonlinear programming, in *Optimization and Control with Applications*, pp. 305–330, Springer.

Skworcow, P., B. Ulanicki, H. AbdelMeguid, and D. Paluszczyszyn (2010), Model predictive control for energy and leakage management in water distribution systems.

Technolog (2014), Regulo, [Online; accessed 05-06-2014].

Todini, E., and S. Pilati (1988), A gradient algorithm for the analysis of pipe networks, in *Computer applications in water supply: vol. 1—systems analysis and simulation*, pp. 1–20, Research Studies Press Ltd.

Ulanicki, B., A. Zehnpfund, and F. Martinez (1996), Simplification of water distribution network models, in *Proc., 2nd Int. Conf. on Hydroinformatics*, pp. 493–500, Balkema Rotterdam, Netherlands.

Ulanicki, B., P. Bounds, J. Rance, and L. Reynolds (2000), Open and closed loop pressure control for leakage reduction, *Urban Water*, *2*(2), 105–114.

Vairavamoorthy, K., and J. Lumbers (1998), Leakage reduction in water distribution systems: optimal valve control, *Journal of hydraulic Engineering*, *124*(11), 1146–1154.

World Health Organization (2004), Design and operation of distribution networks.

Wright, R., I. Stoianov, P. Parpas, K. Henderson, and J. King (2014), Adaptive water distribution networks with dynamically reconfigurable topology, *Journal of Hydroinformatics*, *16*(6), 1280–1301.

699 Yazdani, A., R. A. Otoo, and P. Jeffrey (2011), Resilience enhancing expansion strategies
700 for water distribution systems: A network theory approach, *Environmental Modelling*
701 *& Software*, *26*(12), 1574–1582.

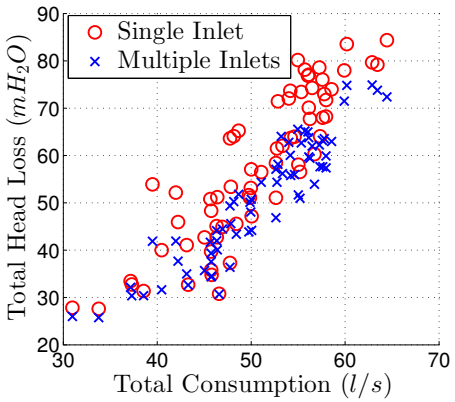

Figure 1. A comparison of head losses at various consumption levels (i.e. stochastic changes in customer demand) for a single and multiple inlet WDN

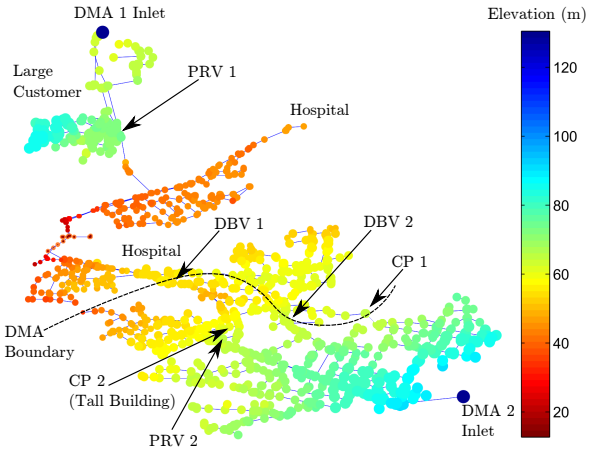

Figure 2. Case study description and elevation plot (m)

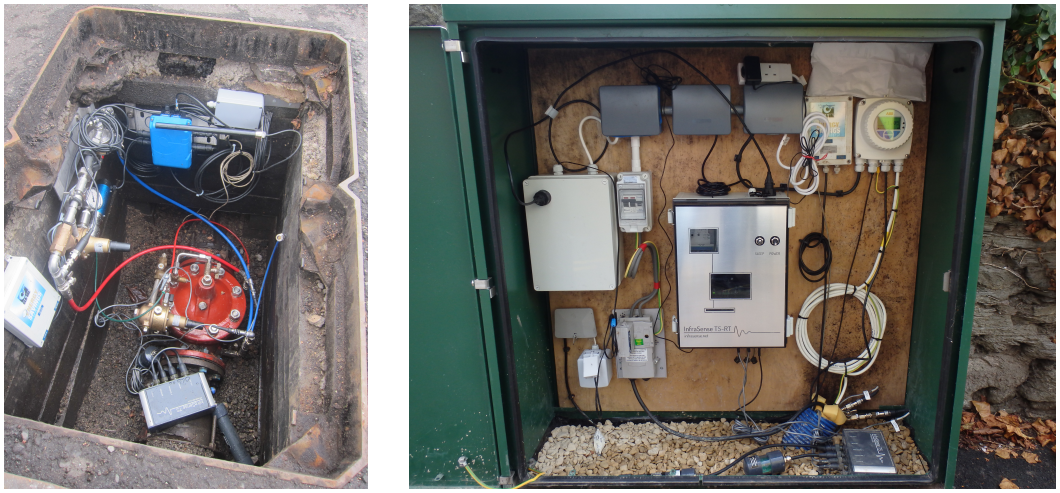

Figure 3. (a) A PRV retrofitted with modulating pilot, turbine for energy harvesting, and antenna for remote comms.(b) Kiosk with real-time pressure and flow communications sampling at 128S/s

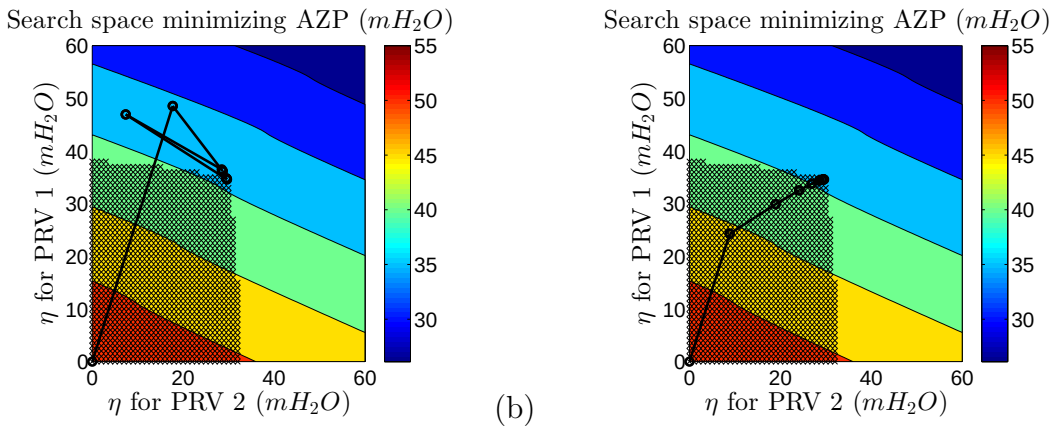

(a) (b)

Figure 4. (a) Cycling in convergence in an infeasible area, (b) Strictly feasible steps to aid convergence

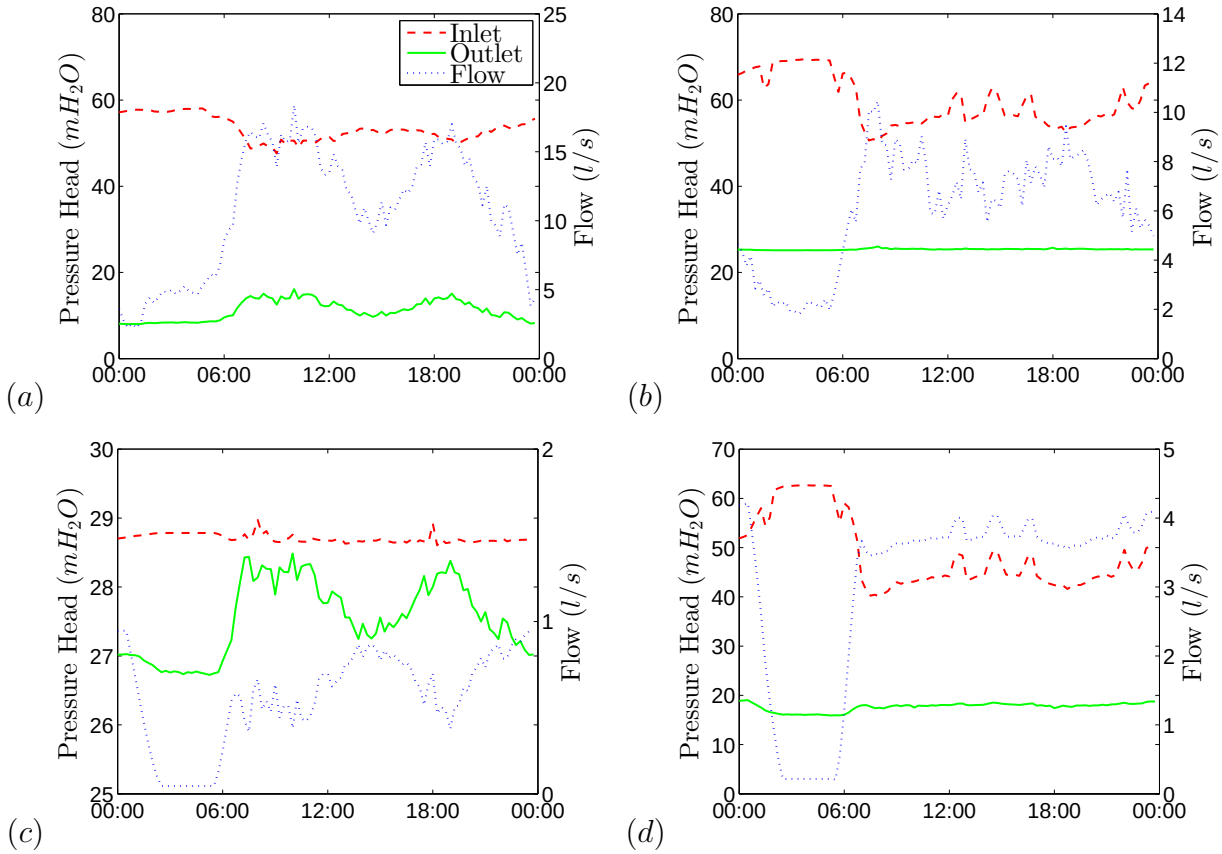

Figure 5. Simulated pressure and flow at (a) PRV 1 (b) PRV2 (c) DBV 1 and (d) DBV 2 for the optimal operation of a dynamic DMA topology

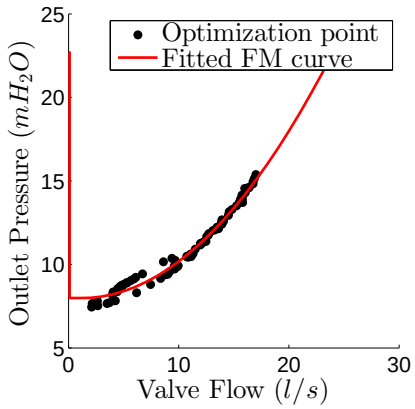

(a)

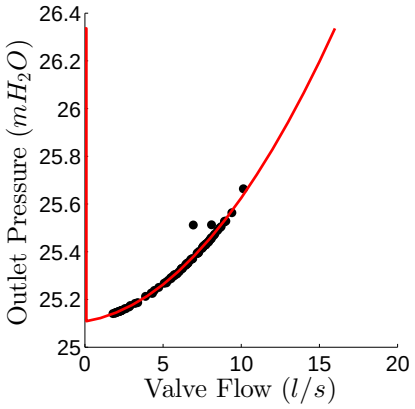

(b)

Figure 6. Fitting of flow modulation curves to the optimization results for (a) PRV 1 and (b) PRV 2

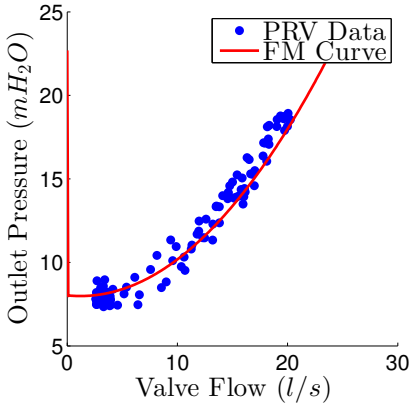

Figure 7. Validation of control actuation at PRV 1 using the acquired pressure data

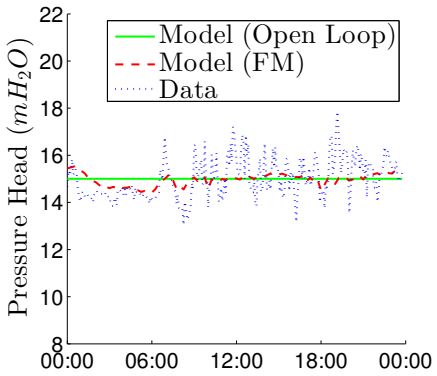

Figure 8. Validation of the hydraulic model and optimization using pressure data at CP 1

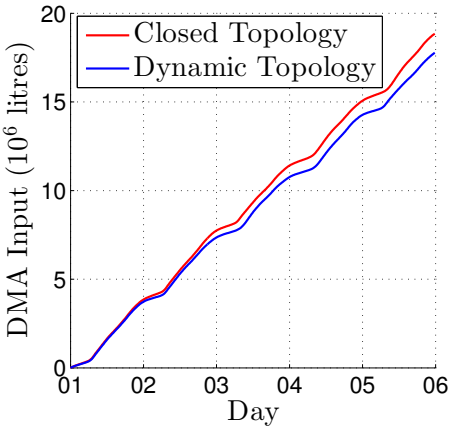

Figure 9. Comparison of water input over a 5 day period for a closed DMA topology with flow modulating PRVs and a dynamic DMA topology

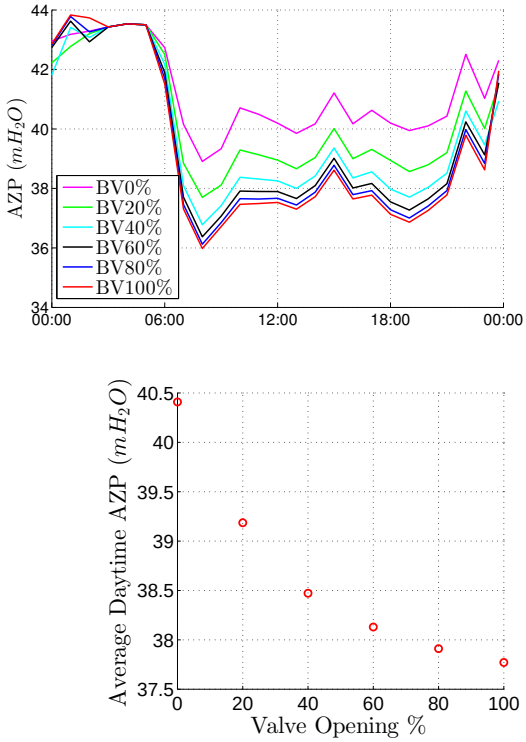

Figure 10. Reducing the AZP further by opening the boundary valves more. Daytime refers to 5am– Midnight